Alterations in oxidative phosphorylation complex proteins in the hearts of transgenic mice that overexpress the p38 MAP kinase activator, MAP kinase kinase 6

Jason A. Wall, Jing Wei, Mimi Ly, Peter Belmont, Joshua J. Martindale, Diem Tran, Jun Sun, Wenqiong J. Chen, Wen Yu, Paul Oeller, Steve Briggs, Asa B. Gustafsson, M. R. Sayen, Roberta A. Gottlieb and Christopher C. Glembotski

Am J Physiol Heart Circ Physiol 291:H2462-H2472, 2006. First published 9 June 2006; doi:10.1152/ajpheart.01311.2005

Am J Physiol Heart Circ Physiol 291: H2462–H2472, 2006.
First published June 9, 2006; doi:10.1152/ajpheart.01311.2005.

Alterations in oxidative phosphorylation complex proteins in the hearts of transgenic mice that overexpress the p38 MAP kinase activator, MAP kinase kinase 6

Jason A. Wall,[1] Jing Wei,[2] Mimi Ly,[1] Peter Belmont,[1] Joshua J. Martindale,[1] Diem Tran,[2] Jun Sun,[2] Wenqiong J. Chen,[2] Wen Yu,[2] Paul Oeller,[2] Steve Briggs,[3] Asa B. Gustafsson,[4] M. R. Sayen,[4] Roberta A. Gottlieb,[4] and Christopher C. Glembotski[1]

[1]*San Diego State University Heart Institute and The Department of Biology, San Diego State University, San Diego;* [2]*Diversa Corporation, San Diego;* [3]*Division of Biological Sciences, University of California-San Diego, La Jolla; and* [4]*Department of Molecular and Experimental Medicine, The Scripps Research Institute, La Jolla, California*

Submitted 13 December 2005; accepted in final form 10 May 2006

Wall, Jason A., Jing Wei, Mimi Ly, Peter Belmont, Joshua J. Martindale, Diem Tran, Jun Sun, Wenqiong J. Chen, Wen Yu, Paul Oeller, Steve Briggs, Asa B. Gustafsson, M. R. Sayen, Roberta A. Gottlieb, and Christopher C. Glembotski. Alterations in oxidative phosphorylation complex proteins in the hearts of transgenic mice that overexpress the p38 MAP kinase activator, MAP kinase kinase 6. *Am J Physiol Heart Circ Physiol* 291: H2462–H2472, 2006. First published June 9, 2006; doi:10.1152/ajpheart.01311.2005.—Ischemia-reperfusion (I/R) has critical consequences in the heart. Recent studies on the functions of I/R-activated kinases, such as p38 mitogen-activated protein kinase (MAPK), showed that I/R injury is reduced in the hearts of transgenic mice that overexpress the p38 MAPK activator MAPK kinase 6 (MKK6). This protection may be fostered by changes in the levels of many proteins not currently known to be regulated by p38. To examine this possibility, we employed the multidimensional protein identification technology MudPIT to characterize changes in levels of proteins in MKK6 transgenic mouse hearts, focusing on proteins in mitochondria, which play key roles in mediating I/R injury in the heart. Of the 386 mitochondrial proteins identified, the levels of 58 were decreased, while only 2 were increased in the MKK6 transgenic mouse hearts. Among those that were decreased were 21 mitochondrial oxidative phosphorylation complex proteins, which was unexpected because p38 is not known to mediate such decreases. Immunoblotting verified that proteins in each of the five oxidative phosphorylation complexes were reduced in MKK6 mouse hearts. On assessing functional consequences of these reductions, we found that MKK6 mouse heart mitochondria exhibited 50% lower oxidative respiration and I/R-mediated reactive oxygen species (ROS) generation, both of which are predicted consequences of decreased oxidative phosphorylation complex proteins. Thus the cardioprotection observed in MKK6 transgenic mouse hearts may be partly due to decreased electron transport, which is potentially beneficial, because damaging ROS are known to be generated by mitochondrial complexes I and III during reoxygenation.

ischemia-reperfusion; mitochondrial complex proteins; mitogen-activated protein

THE MYOCARDIUM CAN BE STRESSED by chronic increases in blood pressure, changes in neurohumoral substances, and ischemia followed by reperfusion (I/R). Numerous signaling pathways, including the mitogen-activated protein kinases (MAPK), are activated in stressed cardiac myocytes; in some cases, those signals foster protection, while in others they mediate damage (5, 22, 24, 42, 46). All three members of the MAPK family are activated during most myocardial stresses; however, the roles played by each in contributing to protection or damage are not entirely clear. For example, p38 MAPK has been reported to have both protective and damaging effects in the myocardium; this conundrum is addressed in recent reviews (1, 24, 31–33) and will, therefore, not be discussed in detail here. However, such apparently conflicting findings raise the possibility that p38 might serve either protective or damaging roles, depending on conditions, such as the cellular and temporal context and differential activation of p38 isoforms.

To begin to examine potential roles for p38 in the myocardium, we determined the effects of overexpressing an upstream activator of p38, MAPK kinase 6 (MKK6). We found that overexpression of MKK6 protected cultured cardiac myocytes against various types of stresses in a p38-dependent manner (54, 55). This protective effect has since been demonstrated by other laboratories, as well (28, 47). In genetically modified mice harboring an α-myosin heavy chain-driven MKK6 transgene, we found that p38 was activated, while neither JNK nor ERK was activated; moreover, ventricular morphology and function were similar to nontransgenic mouse hearts, and the transgenic mice exhibited no overt signs of heart dysfunction or early mortality. However, when exposed to I/R, either ex vivo or in vivo, the MKK6 transgenic mouse hearts exhibited significantly reduced tissue damage and better retention of contractile function (25).

We hypothesized that overexpression of MKK6 might lead to changes in the levels and/or phosphorylation states of p38 and p38-regulated proteins in ways that might contribute to the observed protection. Consistent with this hypothesis were several studies demonstrating that MKK6 transgenic mouse hearts showed increased expression of protective, known p38-regulated proteins (10, 25). However, it is also possible that many other proteins that are not currently known to be p38 regulated may be altered in the transgenic mouse hearts and that these alterations may contribute to the observed protection. In the present study, we addressed this possibility by using a proteomics approach that employed three-dimensional liquid chromatography coupled to tandem mass spectrometry (3D-LC-MS/MS) (49) to assess the relative expression levels of

Address for reprint requests and other correspondence: C. C. Glembotski, The SDSU Heart Institute and the Dept. of Biology, San Diego State Univ., San Diego, CA 92182 (cglembotski@sciences.sdsu.edu).

The costs of publication of this article were defrayed in part by the payment of page charges. The article must therefore be hereby marked "*advertisement*" in accordance with 18 U.S.C. Section 1734 solely to indicate this fact.

proteins in extracts prepared from MKK6 transgenic and nontransgenic mouse heart. This report focuses on proteins in mitochondria because they play a critical role in mediating the damaging effects of I/R. We observed the downregulation of numerous mitochondrial oxidative phosphorylation complex proteins, which are major sites of the generation of the reactive oxygen species (ROS) that mediate I/R injury in the heart. We also found that the MKK6 transgenic mouse hearts exhibited reduced I/R-mediated ROS generation, which may contribute to the protective phenotype in this line. These findings underscore the dynamic nature of the cardiac proteome and demonstrate how functional proteomics studies can provide important insight into the molecular mechanisms underlying the effects of I/R in the heart.

MATERIALS AND METHODS

Animals. Approximately 100 adult mice (*Mus musculus*), 6–8 mo of age, and 25 neonatal rats (*Rattus norvegicus*), were used in this study. All procedures involving animals were in accordance with institutional guidelines. The animal protocol used in this study was reviewed and approved by the San Diego State University Institutional Animal Care and Use Committee.

MKK6 transgenic mice. The transgenic mice used in this study have been described previously (25). All experimental animals were F3 generation or later and were 5–6 mo of age.

Myofibril-depleted cardiac extracts. Myofibril-depleted extracts containing mostly subsarcolemmal mitochondria and cytosolic proteins were prepared as previously described (25).

Reduction, alkylation, and digestion. To control for animal-to-animal variability, myofibril-depleted cardiac extracts were prepared from 10 pooled transgenic and 10 pooled nontransgenic mouse hearts. In preparation for reduction, alkylation, and digestion, proteins in myofibril-depleted cardiac extracts were quantitatively precipitated with ProteoExtract Protein Precipitation Kit (cat. no. 539180, Calbiochem, San Diego, CA) and then resuspended in TNE [50 mM Tris (pH 8.0), 100 mM NaCl, 1 mM EDTA]. RapiGest SF Reagent (cat. no. 186001860; Waters) was added to 2 mg of protein in TNE for a final concentration of 1% RapiGest. Samples were heated and then deglycosylated (cat. no. 362280; Calbiochem) per the manufacturer's protocol. Proteins were then reduced and carboxymethylated with 1 mM TCEP (cat. no. 20490; Pierce Chemical) and 0.5 mg/ml iodoacetamide (cat no. I1149–5g; Sigma Chemical), respectively. Proteins were then digested once with Lys-C (cat. no. 11047825001; Roche) at weight ratio 1:200 (Lys-C:proteins) and twice with trypsin (cat. no. 11047841001; Roche) at weight ratio 1:100 (trypsin:protein). Samples were examined by gel electrophoresis and silver staining to ensure complete digestion. Samples were then treated with 50 mM HCl to degrade the RapiGest and then brought to a pH of 3.0 with NH_4OH. The samples were centrifuged, and the supernatants were removed; the pellets were then resuspended in 70% 2-propanol.

LC-MS/MS. Aliquots of the soluble and insoluble fractions from the nontransgenic and transgenic mouse heart extracts, amounting to 650 μg of protein per aliquot, were fractionated by three-dimensional HPLC (reversed phase; size exclusion; reversed phase) followed by online MS/MS analysis, as previously described (49), with the exception of the following changes in the reversed-phase HPLC elution gradients. For the soluble fractions, the five reverse-phase (RP) gradients used were 0–8% B, 8–20% B, 20–35% B, 35–80% B, and 80–100% B (B = 80% acetonitrile, 19.8% H_2O, 0.2% formic acid), each of which was followed by salt steps of 0, 10, 20, 30, 40, 50, 60, 70, 80, 90, 100, and 1,470 mM ammonium acetate. For the insoluble fractions, the 5 RP gradients used were 0–25% B, 25–40% B, 40–80% B, and 80–100% B, each of which was followed by salt steps of 0, 25, 50, 75, 100, 125, 150, 175, 200, 225, 250, and 2,000 mM ammonium acetate. Eluted peptides were analyzed directly on an LTQ mass spectrometer equipped with a nanospray source (Thermo Finnigan, San Jose, CA). The LTQ mass spectrometer was set to divide the full MS scan into four smaller sections covering a total range of 400–1,800 mass-to-charge ratio. Each of the smaller MS scans was followed by 5 MS/MS scans of the most intense ions from the preceding MS scan. The raw data were then extracted and searched using the SEQUEST program, as previously described (49). By using previously described criteria (48, 51), the results were filtered to obtain the peptide matches and protein identifications. To estimate the frequency of incorrectly matched peptides, the database contained both the forward and reversed mouse sequences. By using this approach, the false hit rate is ~1.3%.

Statistical assessment of MS data. The goal of the proteomics portion of this study was to assess differential expression of proteins in the hearts of transgenic vs. nontransgenic mice but not to assess biological variability between individual animals within a line. Accordingly, we prepared two extracts, one consisting of 10 pooled transgenic mouse hearts and the other consisting of 10 pooled nontransgenic mouse hearts, and two complete proteomics analyses were performed on each extract. This approach has been validated as a method for assessing differential expression when evaluating biological variation is not the goal (23). Proteins that were not identified by at least one spectrum in each of the four runs were removed from further consideration. To account for slight run-to-run differences in MS detection sensitivity, the numbers of spectra observed for a given protein in *runs 1* and *2* were normalized to the total spectra observed in each run. The remaining normalized data were $\log_2$-transformed and assessed for significant differences between transgenic and nontransgenic by using the local-pooled-error (LPE) test (21). This approach provides an estimate of the statistical confidence of the technical replication, not of the biological variation within each extract.

Bioinformatics. The accession ID for each protein, as provided from the SEQUEST search, was used in the web-based Clone/Gene ID Converter, http://idconverter.bioinfo.cnio.es/IDconverter.php to determine gene name, locuslink, and GenBank ID. GOminer was then used (56) to generate a Gene Ontology (GO) association for each gene by using the May 2005 GO database build, and all searches were limited to *Mus musculus*.

Immunoblots. Mitochondrial samples (0.5–1 μg protein per lane) were loaded onto a Bio-Rad 4–12% gel (cat. no. 345–0135; Bio-Rad, Hercules, CA), submitted to SDS-PAGE, and then transferred to polyvinylidene difluoride membranes. Blots were probed for components of the mitochondrial respiratory chain complexes by using monoclonal antibodies specific for each oxidative phosphorylation complex (cat. nos. MS105, MS203, MS304, MS407, and MS507 for complexes I-V, respectively, and as described in more detail in the legend to Fig. 1), or with OXPHOS monoclonal antibody cocktail (cat. no. MS601, Mitosciences, Eugene OR), which cross-reacts with the 20-kDa subunit of complex I, the 30-kDa subunit of complex II, the 50-kDa core2 protein of complex III, cytochrome-*c* oxidase II of complex IV, and ATF synthase F1a of complex V. For normalization purposes, blots were probed with an antibody to α-actinin (cat. no. A7811 Sigma, St. Louis, MO). Blots were then developed using Amersham ECLplus and a Typhoon. Gels were quantified with ImageQuant.

Measurements of respiration of isolated mouse heart mitochondria. Isolation of mouse heart mitochondria and measurement of respiration were performed as described previously (36), with the following modifications. Briefly, mitochondria enriched in subsarcolemmal mitochondria were isolated from mouse hearts by brief Polytron homogenization in ice-cold MSE buffer (200 mM mannitol, 70 mM sucrose, 2 mM EGTA, 5 mM MOPS, pH 7.4) followed by two quick strokes of a loose fit Potter-Elvehjem tissue grinder. Mitochondria were collected by centrifugation at 3,000 *g* following two centrifugations of the homogenate at 600 *g*. All work was performed on wet ice at 0°C. Oxygen consumption was measured at 30°C with a Clark-type oxygen

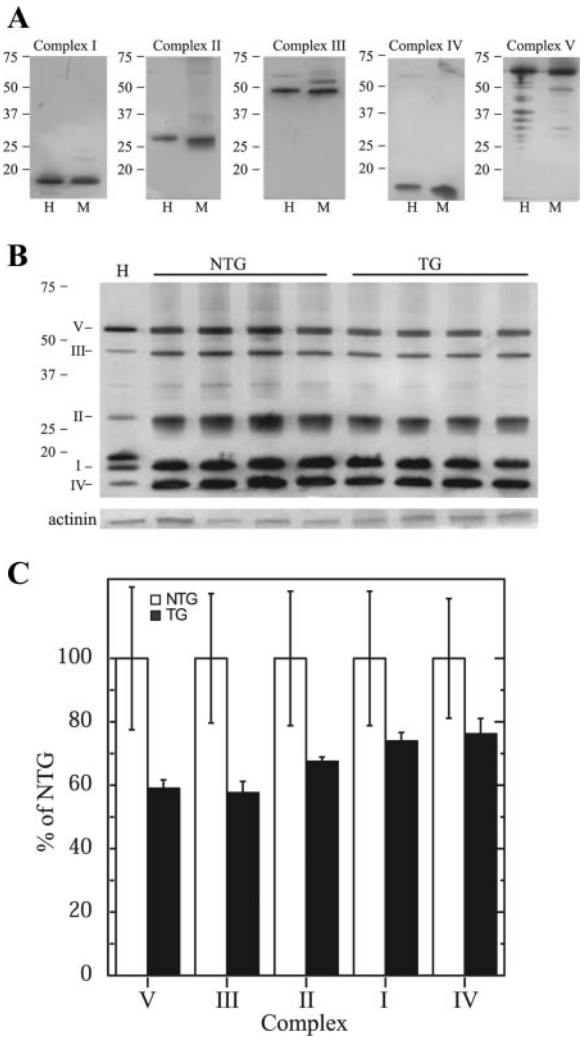

Fig. 1. Analysis of mitochondrial complex proteins. *A:* validation of cytochrome complex antibodies. Mitochondria were isolated from nontransgenic (NTG) and transgenic (TG) mouse hearts ($n = 4$), solubilized and then fractionated by SDS-PAGE (0.5–1 μg of protein per lane), followed by transfer to PVDF and then immunoblotting with individual antibodies that recognize complex I (20-kDa ND6 subunit), complex II (30-kDa FeS, nonheme iron protein, SDHB), complex III (47-kDa core protein 2), complex IV (18-kDa subunit IV), and complex V (55-kDa subunit α-ATP synthase), as described in MATERIALS AND METHODS. A human mitochondrial extract was used as a control (H) to identify subunits in each complex. M = nontransgenic mouse heart mitochondrial extract. The migration positions of molecular mass markers ranging from 20 to 75 kDa are shown on each blot. *B:* decreased mitochondrial complex proteins: cytochrome complex immunoblots. Mitochondria were isolated from NTG and TG mouse hearts ($n = 4$), separated by SDS-PAGE, and blots were probed with a mixture of the antibodies described in *A*. Actinin was used as a loading control. *C:* immunoblot quantification. The immunoblots shown in *B* were quantified as described in MATERIALS AND METHODS.

electrode (Instech) in 600 μl KCl respiration buffer. Complex I and II activity was measured by using 200 μg of mitochondria with palmitoyl-L-carnitine, 40 μM, or pyruvate, 5 mM, as a substrate. Malate was added as a counterion for complex I substrates. Complex II activity was measured with succinate, 5 mM, as a substrate. Complex IV activity was measured by using 100 μg mitochondria with *N*,*N*,*N'*,*N'*-tetramethyl-*p*-phenylenediamine (TMPD), 0.4 mM, and ascorbate, 1 mM, as a substrate. For each complex, the ADP-stimulated respiration rate (state 3) was measured after the addition of 2 mM ADP; the ADP-independent respiration rate, oligomycin-insensitive (state 4), was measured after the addition of 2 μM oligomycin; and the maximal respiration rate was measured after uncoupling the mitochondria with 2 μM FCCP. Data were analyzed by using Student's *t*-test.

Dityrosine formation in mouse hearts. Mouse hearts were cannulated and perfused in Langendorff fashion, as previously described (25), in a darkened apparatus. The perfusion buffer, Krebs-Henseleit buffer (KHB), was supplemented with 0.3 mM L-tyrosine (Sigma T-8566), which reacts with free radicals to form fluorescent dityrosine, which has an excitation at 320 nm and emission of 410 nm (29, 30, 53). Coronary effluent was collected at the end of equilibration and in 30-s intervals during reperfusion. Samples were stored at 4°C in the dark after collection; after all samples for a heart were obtained, 200 μl were loaded into each well of a 96-chamber plate, and absorbance values were read using a Molecular Devices Gemini and SoftMaxPro software. No alterations were observed in samples stored for up to 1 h. Data were collected from five mice from each line, normalized to the equilibration value, and averaged. Statistical analyses were performed by using a one-tailed *t*-test with equal variance.

Superoxide production in mouse hearts. Superoxide production was assessed in hearts following ex vivo I/R via the conversion of dihydroethidium (DHE) to ethidium, as previously described (36). Briefly, frozen hearts were slightly thawed, sliced into 1-mm sections, and incubated with 2 μM DHE for 15 min in the dark. Images of sections were acquired by using an ultraviolet transilluminator and captured by using a Kodak DC120 digital camera with Kodak Digital Science 1D software. Images were analyzed with Adobe Photoshop 7.0, and the percentage of cells exhibiting conversion of DHE (superoxide production) was quantified as the ratio of flourescent pixels to the total heart area.

Mitochondrial swelling assay. Mitochondria were isolated as previously described (25) and resuspended in swelling buffer (10 mM Tris pH 7.4, 120 mM KCl, 20 mM MOPS, 5 mM KH_2PO_4) to a protein concentration of 0.25 μg/μl. Aliquots of 50 μg were used per well in a 96-well plate to which 250 μM Ca^{2+} was added to induce mitochondrial swelling. In some samples, 15 μM cyclosporine A was added to verify that swelling was due to mitochondrial permeability transition pore opening. The absorbance was assessed on a Molecular Devices Versamax plate reader at 520 nM for 30 min after Ca^{2+} addition. Samples were assessed for statistical significance by using a one-way ANOVA with a Student-Newman-Keuls post hoc analysis.

Mitochondrial membrane potential measurement in cultured cardiac myocytes. Neonatal rat ventricular cardiac myocytes (NRVCMs) were isolated and cultured as previously described (27). Cells were then infected by using adenovirus (AdV)-mediated gene transfer of either control, wild-type MKK6 (MKK6wt), or constitutively active MKK6 (MKK6E) constructs, as previously described (18); all strains of AdV used encode a cytomegalovirus-driven green fluorescent protein (GFP) gene, which allowed for the positive identification of infected cells. After 48 h in serum-free medium, cells were subjected to hypoxia (~0.3% O_2 for 10 h) in a glucose- and serum-free medium and then to re-oxygenation (21% O_2 for 21 h) in glucose-containing, serum-free medium, which are conditions that simulate ischemia and reperfusion (sI/R), as it occurs in vivo (27). Cells were then stained with JC-1 (cat. no. T-3168, from Invitrogen-Molecular Probes, Eugene, OR) at a concentration of 1 μg/ml of media for 30 min, after which they were washed three times with serum-free medium and then maintained in minimal media. After 22 h of reoxygenation, green and red images of the cells were captured and analyzed by using Adobe Photoshop. Cells were then scored for those that were infected (GFP positive) and those that retained JC-1 staining. Statistical analysis was performed by using a one-way ANOVA with a Student-Newman-Keuls post hoc analysis.

Superoxide production in cultured cardiac myocytes. Neonatal cardiac myocytes were subjected to simulated ischemia by incubating cells in ischemic buffer (in mM: 125 NaCl, 8 KCl, 1.2 KH_2PO_4, 1.25 $MgSO_4$, 1.2 $CaCl_2$, 6.25 $NaHCO_3$, 20 2-deoxyglucose, 5 Na-lactate,

20 HEPES, pH 6.6) and placing the dishes in hypoxic pouches (GasPak EZ, BD Biosciences). After 2 h, reperfusion was started by changing to Krebs-Henseleit buffer (in mM: 110 NaCl, 4.7 KCl, 1.2 KH_2PO_4, 1.25 $MgSO_4$, 1.2 $CaCl_2$, 25 $NaHCO_3$, 15 glucose, 20 HEPES, pH 7.4) containing 2 μM DHE. After 45 min of reperfusion, intracellular superoxide production was assessed by measuring changes in fluorescence resulting from DHE oxidation to yield fluorescent ethidium. Cells were observed with a Nikon TE300 fluorescence microscope (Nikon), and images were captured by using a cooled CCD camera (Orca-ER, Hamamatsu). At least 200 cells were scored from two replicate dishes in three independent experiments.

RESULTS

Myofibril-depleted mouse ventricular proteome. Because of their relatively high abundance in the heart, it was determined that myofibril-related proteins would reduce our ability to detect lower abundance proteins. Accordingly, because they were not the focus of this study, we used a previously described fractionation procedure (25) to prepare myofibril-depleted extracts. We then carried out LC-MS/MS analyses of extracts prepared from nontransgenic and MKK6 transgenic mouse hearts, as described in MATERIALS AND METHODS. The proteins identified using SEQUEST were sorted into GO categories on the basis of their functions and subcellular locations (56), as described in MATERIALS AND METHODS. In this study, we focused on proteins in the mitochondria because they are known to play a critical role in mediating the effects of I/R.

We observed spectra for 386 mitochondrial proteins. However, for 161 of the 386, fewer than one spectrum was observed in at least one of the four analyses; because of this low spectral count, these proteins were not retained for statistical analyses. Thus the remaining 225 mitochondrial proteins were assessed for statistical differences between the two mouse lines, by using a procedure similar to a previously published method (7), which validated the use of LC-MS/MS spectral data to compare the levels of a protein in control vs. treated samples. Using this method, we estimated that there was no statistical difference in the levels of 165 of the 225 mitochondrial proteins in nontransgenic and transgenic mouse hearts (see Table 1). However, 60 of the 225 mitochondrial proteins were estimated to be present at significantly different levels, with 58 proteins being decreased and 2 exhibiting increases in the transgenic mouse hearts (see Table 2). We were surprised to find 21 proteins involved in oxidative phosphorylation among the 58 proteins that were decreased (see Table 2, *rows 1–21*). Alterations in the levels of certain oxidative phosphorylation complex proteins have been shown to reduce the assembly of the complexes (45). Accordingly, immunoblots were carried out by using monoclonal antibodies directed against portions of each of the mitochondrial oxidative phosphorylation complexes. Control immunoblots demonstrated that subunits from each of the five mitochondrial complexes in nontransgenic mouse heart mitochondria cross-reacted with the appropriate antibodies and migrated to the same positions as the corresponding subunits in a commercially available control human cell mitochondrial preparation (Fig. 1*A*). When blots were probed with a mixture of all five antibodies, transgenic mouse heart mitochondria exhibited decreases of 20–40% in the levels of components in complexes I, II, III, IV, and V (Fig. 1, *B* and *C*). These findings support the proteomics results, providing additional data using different methods that mitochondrial oxidative phosphorylation complex levels are decreased in the transgenic mouse hearts.

Mitochondrial respiration, ROS, and mitochondrial membrane potential. To further validate the proteomics and immunoblot results, we examined potential physiological consequences of decrease in mitochondrial oxidative phosphorylation complex proteins. We hypothesized that transgenic mouse heart mitochondria would display decreased respiration rates. Accordingly, electron transfer capacities of isolated mitochondria were assessed, as previously described (36); representative tracings are shown in Fig. 2*A*. Compared with nontransgenic mice, respiration rates of mitochondria isolated from transgenic mice were impaired when substrates for complexes I (palmitoyl carnitine), II (succinate), or IV (TMPD/ascorbate) were used. We found that state 3, state 4 (not shown), and FCCP-uncoupled, maximal respiration were reduced by 30–50% in the MKK6 transgenic mitochondria (Fig. 2, *B* and *C*). These results provide a functional validation of the observed changes in the mitochondrial complex proteome in MKK6 transgenic mouse hearts.

On reperfusion, ROS are generated by complexes I and III (17, 41, 44). Because the MKK6 transgenic mice exhibited decreases in several complex I and III proteins, we hypothesized that, compared with nontransgenic, they would also generate less ROS. Accordingly, free radical generation was measured in isolated perfused mouse hearts from both mouse lines. After 2 min of reperfusion, we found that compared with transgenic, the nontransgenic mouse hearts exhibited a significant increase in free radical generation, as measured by dityrosine formation (Fig. 3*A*). The generation of superoxide in mouse hearts after 30 min of ischemia and 15 min of reperfusion was measured by conversion of dihydroethidium (DHE) to ethidium. We found that, compared with transgenic mice, the nontransgenic mouse hearts subjected to I/R exhibited a significant increase in DHE conversion (Fig. 3*B*). Taken together, these results suggest that during I/R, MKK6 transgenic mouse heart mitochondria generate less ROS than nontransgenic mouse hearts.

ROS are among several factors that increase during reperfusion that can stimulate the opening of the mitochondrial permeability transition pore (MPTP) (16). Because the transgenic mouse heart mitochondria exhibited lower rates of ROS generation, we hypothesized that they might also exhibit reduced MPTP activation. Accordingly, mitochondria were isolated from the hearts of both mouse lines, and Ca^{2+}-induced MPTP opening was assessed by measuring mitochondrial swelling (2). On treatment with Ca^{2+}, we observed a more rapid decrease in absorbance of the nontransgenic mouse heart mitochondria than transgenic, suggesting that compared with nontransgenic, the MKK6 transgenic mice exhibit reduced Ca^{2+}-stimulated MPTP activation.

Effects of MKK6 overexpression in primary cardiac myocytes. We next evaluated whether MKK6 overexpression in isolated cardiac myocytes affected mitochondrial function. Accordingly, primary neonatal rat ventricular myocytes were infected with a recombinant adenoviral strains that encode either MKK6wt or MKK6E (18). The cells were then exposed to sI/R, as previously described (27). The status of the mitochondrial membrane potential, which is an estimate of the electrochemical gradient across the inner mitochondrial membrane, and thus MPTP opening, was assessed with the fluores-

cent dye JC-1, as previously described (8, 11). After sI/R, there was a reduction in the number of cells able to retain the mitochondrial membrane potential in cultures infected with the control AdV, while cells infected with AdV-MKK6wt or AdV-MKK6E exhibited very little change in mitochondrial membrane potential (Fig. 4*A*). The generation of superoxide was also examined in the cultured cardiac myocytes, where we found significantly lower rates of DHE conversion in AdV-MKK6wt- and AdV-MKK6E-infected cultures compared with those infected with the control AdV (Fig. 4*B*). Although the neonatal cardiac myocytes do not necessarily represent all aspects of the adult myocyte phenotype, these results indicate that in cultured cardiac myocytes, overexpression of either MKK6wt or MKK6E confers some of the same characteristics observed in MKK6 transgenic mouse hearts, including reduced ROS generation and retention of the mitochondrial membrane potential.

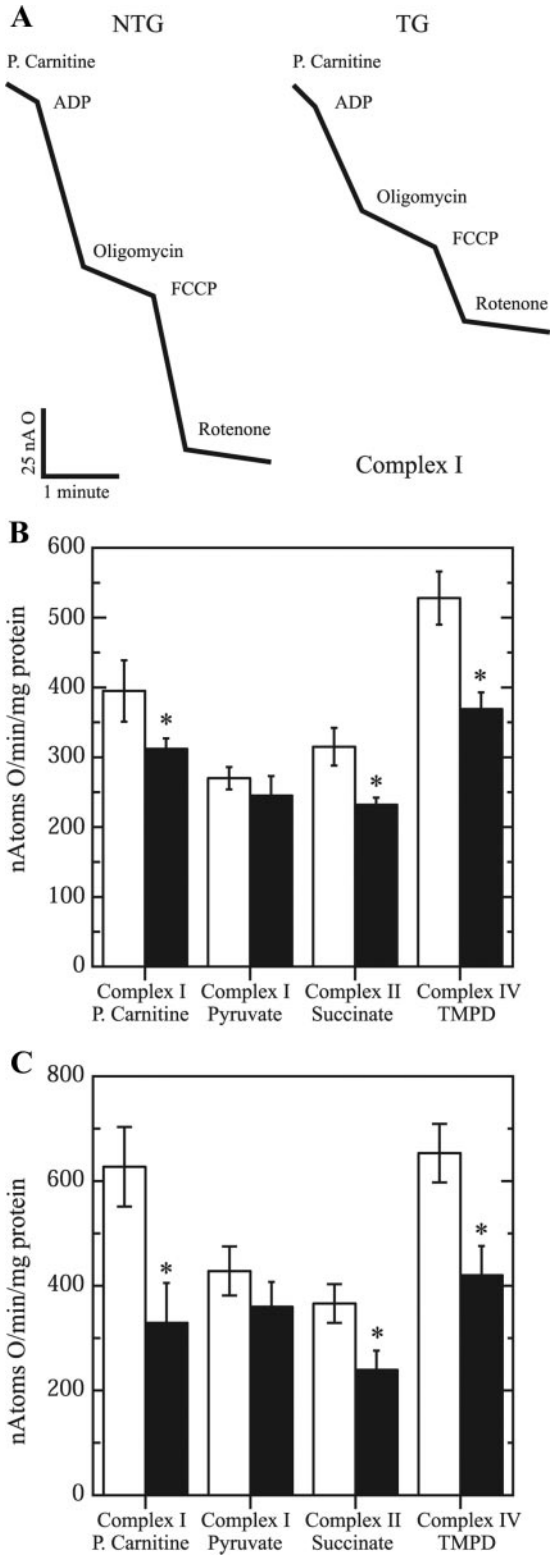

Fig. 2. Respiration studies of mitochondria isolated from MAPK kinase 6 (MKK6) TG and NTG mouse hearts. *A*: representative O_2 electrode tracings obtained with NTG and TG mouse heart mitochondria are shown. Scale indicates nA O_2 consumed per unit time. Each tracing represents the data obtained from mitochondria pooled from 2 mouse hearts. Inflections represent changes in respiration rates observed on addition of the compounds shown. *B*: state 3 respiration rates. The respiration rates were determined from tracings similar to those shown in *A* after the addition of the substrates shown, which allows the estimation of electron transport in complexes I, II, and IV. State 3 respiration is the rate obtained after the addition of 2 μM ADP. Data are shown as the means of $n = 5$ independent analyses of mitochondria from 10 TG and 10 NTG mouse hearts SD. *NTG different from TG, $P \leq 0.05$, as determined by using Student's *t*-test. *C*: maximal respiration rates. The respiration rates were determined as described in *B*. Maximal respiration is the rate obtained after the addition of 2 μM FCCP. Data are shown as means ($n = 5$ independent analyses of mitochondria from 10 TG and 10 NTG mouse hearts) ± SD. *NTG different from TG, $P \leq 0.05$, as determined by using Student's *t*-test.

DISCUSSION

In the present study we found that 21 mitochondrial oxidative phosphorylation complex proteins, 24 proteins involved in fatty acid oxidation (FAO), and 2 proteins of the pyruvate dehydrogenase complex were reduced in MKK6 transgenic mouse hearts (Fig. 5). We also found that several proteins involved in apoptosis, mitochondrial biogenesis, and ROS metabolism were decreased (Table 2). Because of the I/R-protective phenotype exhibited by MKK6 transgenic mouse hearts and the central role played by certain oxidative phosphorylation proteins in generating the ROS that can mediated I/R damage, we focused our analyses in this study on the oxidative phosphorylation proteins.

We observed decreased levels of each of the five mitochondrial complexes in the MKK6 transgenic mouse heart mitochondria when examined by immunoblotting (Fig. 1) and decreases in complexes I, III, and V in the proteomics analysis (Table 2 and Fig. 5). Complex I, which is also known as NADH ubiquinone oxidoreductase, or NADH dehydrogenase, is comprised of 46 subunits, and at 950 kDa, it is the largest of the respiratory chain components (6). Complex I catalyzes electron entry into electron transport from NADH that is derived from the TCA cycle and fatty acid oxidation (Fig. 5). In the MKK6 mouse hearts, we observed 11 proteins that were decreased, two of which were Ndufs1 and 4. Decreases in the levels of Ndufs4 and Ndusf1 have been found to reduce the levels of the holocomplex I and to result in reduced electron transport and ROS generation on hypoxia or reoxygenation (20). This is consistent with our findings that complex I-mediated oxygen utilization was reduced (Fig. 2) and that the generation of ROS upon reperfusion of hearts or reoxygenation of cultured cardiac myocytes was reduced (Figs. 3 and 4). Moreover, Nudufs1 and Nudufs2 are the core subunits that are

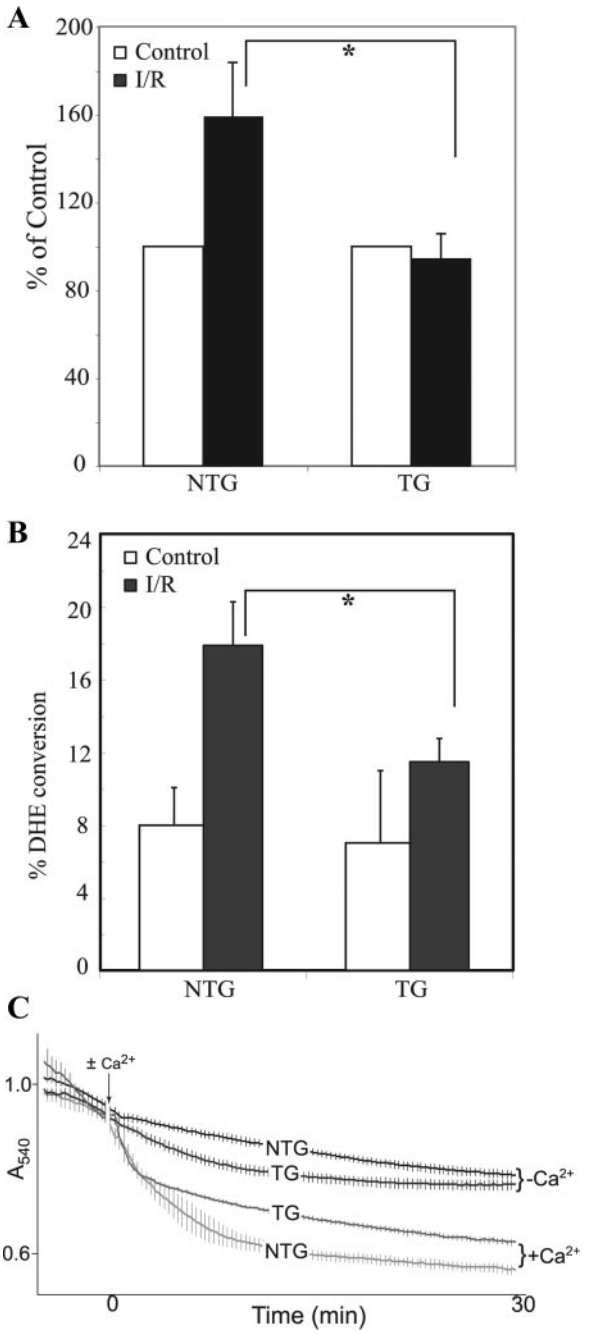

Fig. 3. Analyses of free radical generation and mitochondrial swelling. *A*: dityrosine formation. Hearts from NTG or TG mice were perfused ex vivo for either 27 min (control; $n = 5$ from each line) or for 25 min of global ischemia followed by 2 min of reperfusion (I/R; $n = 5$ from each line). Free radical release was estimated by measuring dityrosine generation, as described in MATERIALS AND METHODS. Results are means ± SE. *Different from value shown, $P \leq 0.05$, as determined using Student's *t*-test. *B*: superoxide production. Hearts from NTG or TG mice ($n = 3$ from each line) were perfused ex vivo for either 45 min (control) or for 30 min of global ischemia, followed by 15 min of reperfusion (I/R). Hearts were then analyzed for superoxide production by dihydroethidium (DHE) conversion, as described in MATERIALS AND METHODS. Results are means ± SE. *Different from value shown, $P \leq 0.05$, as determined using Student's *t*-test. *C*: mitochondrial swelling. Mitochondria were isolated from NTG and TG mouse hearts, and the rate of swelling after addition of 250 μM Ca was determined as described in MATERIALS AND METHODS. Ca-stimulated mitochondrial swelling was inhibited by cyclosporine A (not shown), confirming that this measurement represented an estimation of mitochondrial permeability transition pore opening. Results are means ($n = 5$ hearts from each line) ± SE. *Different from values shown, $P \leq 0.05$, as determined by using Student's *t*-test.

essential for electron transfer from NADH to ubiquinone and for the generation of the protonmotive force (6). Because we observed reductions in both Nudufs1 and 2, we would expect that proton pumping would also be impaired in MKK6 mouse heart mitochondria. Although we did not examine pyridine nucleotide levels, given the central roles metabolic roles of NADH in carrying electrons from the TCA cycle and FAO to complex I (Fig. 5), reduction of complex I in the transgenic mouse hearts would be expected to decrease the rates of NADH oxidation in the MKK6 mouse mitochondria.

Complex II, also known as succinate-ubiquinone oxidoreductase, or succinate dehydrogenase, is composed of four subunits and participates in both electron transport and the TCA cycle. Although we did not observe reductions in any complex II proteins that reached statistical significance in the proteomics analysis, we detected reduced levels of subunit b of succinate dehydrogenase (Sdhb) by immunoblotting (Fig. 1). Although few studies have examined the effects of decreased complex II, as expected, this complex has been shown to be rate limiting for succinate oxidation (4), consistent with our observations that the MKK6 transgenic mouse heart mitochondria exhibit reduced respiration when succinate is provided as a carbon source (Fig. 2).

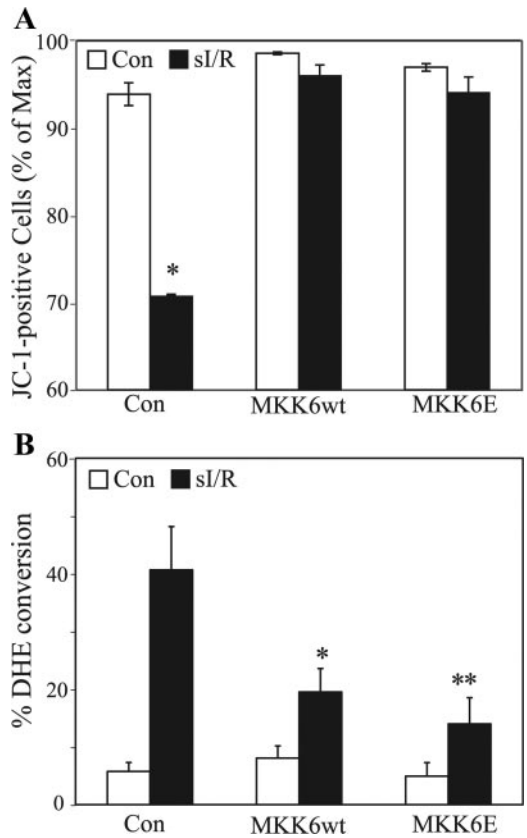

Fig. 4. Effect of wild-type MKK6 (MKK6wt) or constitutively active MKK6 (MKK6E) overexpression in cultured cardiac myocytes. Primary neonatal rat ventricular myocytes were infected with adenovirus (AdV)-control (Con), AdV-MKK6wt, or AdV-MKK6E and then treated ± simulated ischemia/reperfusion (sI/R) and analyzed for mitochondrial membrane potential (*A*) or for superoxide formation (*B*) as described in MATERIALS AND METHODS. Results are means ± SE. *$P < 0.05$, **$P < 0.01$, different from control as determined by using Student's *t*-test.

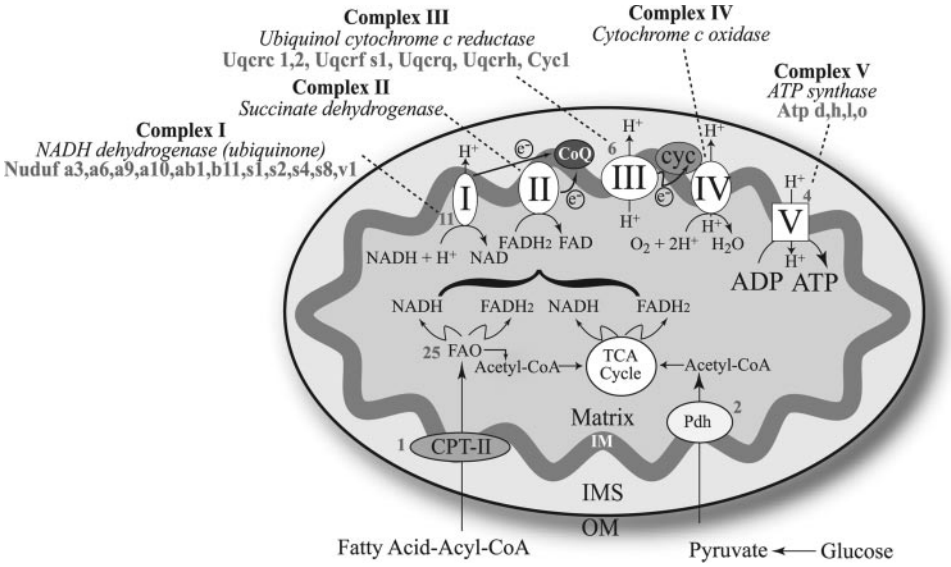

Fig. 5. Diagram of mitochondrial metabolism proteins changed in the MKK6 transgenic mouse hearts. The basic roles of fatty acid oxidation (FAO) and the tricarboxylic acid (TCA) cycle in generating NADH and $FADH_2$ for electron transport are shown. Also shown are the five oxidative phosphorylation complex proteins (I, II, III, IV, and V), as well as cyctochrome *c* (cyc), the flow of electrons through the complexes, and the generation of ATP by complex V. The numbers of proteins exhibiting decreased expression levels in pyruvate dehydrogenase (Pdh), fatty acid uptake [carnitine palmitoyl transferase (CPT)-I and -II], FAO, and each of the cytochrome complexes are shown. The name of each cytochrome complex is shown in italics and the symbols of each subunit changed in each complex are shown beneath the complex name; full names of each subunit can be found in Table 2. IM, inner mitochondrial membrane; IMS, intermembrane space; OM, outer mitochondrial membrane. Decreases in these proteins would be expected to affect oxidative respiration in the transgenic mouse heart mitochondria as described in DISCUSSION.

Complex III, also known as ubiquinol-cytochrome *c* oxidoreductase, is composed of 11 subunits and catalyzes electron transfer from reduced ubiquinone to cyctochrome *c*. The proteomics analysis indicated that six complex III subunits were reduced in the MKK6 mouse hearts. Two of the complex III proteins that were reduced were Uqcrc1 and Uqcrc2, which are also known as ubiquinol cytochdrome *c* reductase core proteins 1 and 2. Uqcrc1 and 2 mediate the formation of the complex between cytochromes *c* and *c*1, and they are believed to be the primary site of ROS generation by reverse electron transport during hypoxia as well as reoxygenation (15). This is consistent with our findings of increased ROS generation in the MKK6 mouse hearts and cultured cells on reoxygenation. The cytochrome *c*-1 (cyc1) subunit of complex III accepts electrons from Uqcrfs1, which is also known as Rieske iron-sulfur polypeptide I, and transfers them to soluble cytochrome *c* (37, 38); cyc1 and Uqcrfs1 were both reduced in the MKK6 mouse hearts (Table 2), which is likely to cause reduced electron flow-coupled proton translocation and thus decrease the overall activity of complex III (50).

Complex IV, also known as cytochrome *c* oxidase, is composed of 13 different subunits; cytochrome *c* shuttles electrons from complex III to complex IV. Although we did not observe any reduction in cytochrome *c* or any complex IV proteins in the proteomics analysis, the immunoblot showed a reduction of subunit IV of complex IV (Fig. 1), suggesting that electron flow from complex III to IV would be impaired in the transgenic mouse hearts examined in this study.

We also observed reduced levels of Atp5l and Atp5h of complex V, both of which are subunits of the transmembrane F_0, proton transport mediating portion of F_1F_0 ATP synthase (Fig. 5) (13). Moreover, there was a reduction in the levels of the Atp5d and Atp5o of complex V, which are subunits of the F_1 complex of ATP synthase that constitutes the catalytic site of the enzyme. Given the reductions in the levels of these four important ATP synthase subunits, we would expect decreased proton transport, as well as ATP generation in the MKK6 transgenic mouse heart mitochondria. We have yet to directly measure ATP generation, and while we have not observed any overt reduction of contractile performance in the MKK6 transgenic mouse hearts, they do exhibit a slightly lower resting heart rate, as well as marginally reduced fractional shortening (25), which could be clues that contractility is compromised. Nonetheless, the MKK6 transgenic mice, which do not display altered life spans, do not exhibit any overt effects of reduced oxidative respiration, nor are the hearts abnormal in terms of gross or microscopic histology or nonexercised function. Future studies examining ATP generation in MKK6 transgenic mouse hearts, as well as the effects of exercise on cardiac function and performance, will be required to address possible detrimental effects of the reduced oxidative respiration.

It is of interest to consider how MKK6-mediated p38 activation might cause a reduction in oxidative phosphorylation complex protein expression. The expression of most oxidative phosphorylation complex proteins is regulated by nuclear factors (NRF) 1 and 2, as well as PGC-1α, all of which coordinate with peroxisome proliferator-activated receptor (PPAR)-α and PPAR-β to induce the transcription of many nuclear genes that encode mitochondrial proteins (14, 19). However, to the best of our knowledge, p38-mediated decreases in the levels of oxidative phosphorylation complex proteins have not been observed. In fact, there is evidence to the contrary, suggesting that p38 actually increases the expression of oxidative phosphorylation complex proteins. For example, p38 can phosphorylate PGC-1α, as well as p160 myb binding protein, a PGC-1α suppressor; these phosphorylation events increase PGC-1α-mediated coactivation of PPAR-α-dependent gene induction, which leads to increased levels of oxidative phosphorylation proteins (3, 12). Perhaps the decreases in oxidative phosphorylation protein levels we observed are not actually mediated through the PPARs and PGC-1α but instead involve other transcription factors. For example, Sp1 represses expression of certain oxidative phosphorylation protein genes (34). p38 has been shown to activate Sp1 in macrophages (52), vascular smooth muscle cells (26), and fibroblasts (9), suggesting a possible mechanism by which MKK6-activated p38 might depress oxidative phosphorylation protein levels in the transgenic mouse hearts examined in the present study. Addition-

Table 1. *Unchanged mitochondrial proteins*

	1	2	3	4	5	6	7
	NTG		NTG	TG		TG	
	1	2	Ave	1	2	Ave	Symbol
1	3346	2716	3031	2610	2194	2402	Atp5a1
2	2746	3445	3096	2282	2294	2288	Atp5b
3	1582	1819	1701	1604	2126	1865	Aco2
4	1130	958	1044	842	708	775	Etfa
5	883	844	863	650	470	560	Mdh2
6	846	814	830	980	1176	1078	Gapd
7	819	673	746	492	493	493	Vdac1
8	713	599	656	581	595	588	Ak1
9	569	592	581	422	416	419	Hadhb
10	565	607	586	369	388	379	Cs
11	563	606	585	407	445	426	Acadm
12	443	445	444	536	441	488	Got2
13	411	342	376	446	330	388	Hspa9a
14	386	408	397	453	407	430	Ogdh
15	354	491	422	446	378	412	Pkm2
16	341	216	279	246	171	209	Dlst
17	320	300	310	264	593	428	Slc25a5
18	304	277	290	274	224	249	Cycs
19	302	302	302	244	222	233	Dld
20	281	261	271	440	404	422	Hspcb
21	272	274	273	223	224	224	Fh1
22	263	273	268	230	285	257	Acadl
23	258	283	270	181	223	202	1700007H16Rik
24	240	293	267	282	333	307	Ckb
25	218	190	204	190	195	193	Trygn16
26	207	287	247	264	272	268	Idh3a
27	198	147	173	144	205	175	Hspe1
28	188	171	179	161	188	174	Suclg1
29	170	100	135	89	85	87	Dlat
30	169	151	160	147	110	128	Cox4i1
31	165	151	158	113	136	124	Acat1
32	156	159	158	144	123	134	Prdx5
33	146	127	137	93	117	105	Slc25a3
34	144	230	187	181	160	170	Gbas
35	140	182	161	79	130	105	Cox5a
36	139	166	152	143	219	181	2300002G02Rik
37	127	106	117	134	108	121	Pdha1
38	120	63	92	64	48	56	2410011G03Rik
39	119	143	131	144	171	158	Atp5c1
40	117	161	139	166	139	153	Dci
41	116	142	129	191	168	180	Prdx6
42	108	116	112	156	86	121	C1qbp
43	105	61	83	67	34	50	Ppif
44	94	72	83	56	47	52	Etfdh
45	92	33	63	82	71	76	Ywhaz
46	84	85	85	116	101	108	Ctsd
47	79	79	79	59	48	53	Vdac2
48	76	58	67	60	58	59	Cox5b
49	76	84	80	125	73	99	Acsl1
50	74	59	67	44	40	42	D10Jhu81e
51	71	83	77	90	84	87	Idh3b
52	69	41	55	75	67	71	Hspa2
53	69	65	67	32	84	58	Slc25a13
54	66	78	72	56	52	54	Nme2
55	65	42	53	30	29	29	Immt
56	64	79	71	78	93	85	Prdx3
57	55	32	44	26	21	24	Ndufa4
58	54	85	70	61	64	63	Bcat2
59	54	58	56	95	64	79	Tubb3
60	45	74	60	88	61	74	Idh3g
61	41	46	43	23	34	28	Ndufs5
62	40	52	46	48	39	44	Dbi
63	39	63	51	30	24	27	Acas2l
64	39	40	40	23	35	29	Ndufs7
65	39	30	34	31	28	29	1110025H10Rik
66	38	28	33	32	24	28	2610207I16Rik
67	38	47	42	32	29	30	Pcca
68	37	27	32	16	22	19	Ak2
69	35	58	47	26	31	29	Sdhb
70	33	9	21	38	20	29	Txn1
71	30	21	26	18	18	18	D10Ertd214e
72	30	35	32	39	31	35	Mrps36
73	29	52	41	60	54	57	Ckmt1
74	29	26	28	14	12	13	Letm1
75	29	41	35	40	43	41	Cat
76	27	26	26	20	13	17	Dbt
77	26	16	21	29	12	21	Lap3
78	24	19	21	14	10	12	Pccb
79	23	20	21	18	13	16	Mccc1
80	23	21	22	13	13	13	Uqcrb
81	22	27	25	14	12	13	Txn2
82	19	14	16	38	13	26	Dnm1l
83	18	26	22	21	6	13	Ndufa7
84	18	59	38	18	24	21	Ndufa8
85	16	16	16	13	8	10	Opa1
86	15	9	12	14	7	10	Atp5k
87	15	12	14	26	17	21	Nfs1
88	14	2	8	6	2	4	Ak4
89	14	5	10	11	7	9	Lrpprc
90	13	12	13	6	4	5	D630032B01Rik
91	13	7	10	6	4	5	Ndufa2
92	13	26	20	37	20	29	Ndufb8
93	13	6	9	14	8	11	2410002K23Rik
94	13	28	21	12	8	10	Grim19
95	12	19	15	8	19	14	Hba-a1
96	11	21	16	14	3	9	1500032D16Rik
97	11	5	8	8	1	5	Atp5j2
98	11	14	12	8	7	7	D16H22S680E
99	11	2	7	9	7	8	Diablo
100	11	15	13	15	15	15	Hk1
101	11	1	6	4	1	2	Mtx2
102	11	14	12	17	9	13	Psmc3
103	10	9	9	16	4	10	Cox6a1
104	10	4	7	3	2	2	Rtn4ip1
105	9	7	8	11	2	7	Coq3
106	9	1	5	5	6	6	Cox7a2l
107	8	23	16	4	12	8	Cox6a2
108	8	9	9	1	1	1	H2-Ke6
109	8	6	7	4	2	3	Stoml2
110	8	6	7	5	2	4	1810004I06Rik
111	8	5	6	5	1	3	Bcl2l13
112	8	6	7	5	1	3	Echdc3
113	8	4	6	5	13	9	Nol3
114	8	4	6	2	1	1	Tomm22
115	8	9	8	10	4	7	Txnrd2
116	7	4	5	5	3	4	2310050B20Rik
117	7	5	6	9	7	8	2900070E19Rik
118	7	19	13	15	11	13	Crat
119	7	6	6	6	4	5	D530020C15Ri
120	7	2	5	1	1	1	Fdx1
121	7	5	6	7	10	9	Gsr
122	6	2	4	6	2	4	Akr7a5
123	6	12	9	9	7	8	Auh
124	6	6	6	5	9	7	Cyb5
125	6	11	9	11	8	9	D16Ertd502e
126	6	7	7	5	1	3	Ndufb4
127	6	6	6	7	4	6	Pitrm1
128	6	4	5	2	1	1	Prkaca
129	5	2	4	3	2	2	A930009M04R
130	5	1	3	2	2	2	Gstz1
131	5	2	4	4	2	3	Hsd17b4
132	5	5	5	7	10	9	Lypla1
133	5	1	3	4	1	2	Mtch2
134	4	1	3	1	1	1	Abcd3
135	4	1	3	1	1	1	Amacr
136	4	10	7	9	2	6	Atp5j
137	4	5	5	6	8	7	Clic4
138	4	2	3	1	1	1	Hadh2
139	4	12	8	4	6	5	Ndufa5
140	4	2	3	3	1	2	Ndufb5
141	4	4	4	4	2	3	Pdk2
142	4	1	3	3	4	4	Timm44
143	3	4	4	5	1	3	Atad3a
144	3	2	3	5	1	3	Dnaja3
145	3	5	4	1	1	1	Ethe1
146	3	5	4	5	1	3	Pcx
147	3	4	4	2	1	1	Tomm40
148	3	1	2	3	1	2	2810435D12Rik
149	3	2	2	5	2	4	Atp6v1a1
150	3	6	4	2	2	2	Cyct
151	3	10	6	8	3	6	Grpel1
152	3	5	4	2	3	3	Ndufb3
153	3	22	12	22	6	14	Prdx4
154	3	4	3	4	1	2	Sqrdl
155	3	4	3	7	2	5	Vars2
156	2	2	2	3	1	2	1810044O22Rik
157	2	4	3	1	2	2	Frda
158	2	1	1	1	1	1	Mrps18b
159	2	2	2	2	1	1	Slc25a22
160	1	1	1	4	1	2	Afg3l1
161	1	1	1	3	2	2	Bckdk
162	1	5	3	7	3	5	Cbr2
163	1	1	1	5	8	7	D430026P16Rik
164	1	1	1	1	2	2	Dhodh
165	1	5	3	5	4	4	Glul

The 165 mitochondrial proteins that did not exhibit significant differences between transgenic (TG) and nontransgenic (NTG) mice [i.e., local pooled error (LPE) ≥ 0.05] are shown. Nos. of spectra observed for each protein, normalized as described in MATERIALS AND METHODS, are shown for the two NTG analyses (*columns 1* and *2*) and the two TG analyses (*columns 4* and *5*). The proteins in this table were sorted by numbers of spectra observed in NTG *run 1* (*column 1*). The only proteins shown are those for which at least 1 spectrum was observed in each of the 4 analyses. *Columns 3* and *6* are the averages of *columns 1 and 2* and of *columns 4* and *5*, respectively. *Column 7* shows the gene symbol, as found by Mouse Genome Informatics search at http://www.informatics.jax.org/.

ally, it may be possible that MKK6-mediated effects on oxidative phosphorylation protein levels could also be indirect and/or posttranscriptional.

The reduction of oxidative phosphorylation proteins in the transgenic mouse hearts is qualitatively similar to that observed in failing hearts, where there is a shift in mitochondrial substrate utilization from primarily fatty acid β-oxidation (FAO) in the healthy heart, to glucose oxidation in the diseased heart (35, 39, 40, 43). This metabolic shift has been considered by some to contribute to the failing heart phenotype; however, others believe that it may be an adaptive response that allows for preserved ATP generation during times when mitochondrial oxidative phosphorylation is reduced. Because this shift is commonly associated with a reduction in the levels of the proteins responsible for FAO, it is of interest that 26 of the 60 changed mitochondrial proteins in MKK6 transgenic mouse hearts are involved in fatty acid transport into the mitochondrion and FAO (see Table 2 and Fig. 5); 24 of those 26 FAO

Table 2. *Significantly changed mitochondrial proteins*

	1	2	3	4	5	6	7	8	9	10	11
	NTG		NTG	TG		TG					
	1	2	Ave	1	2	Ave	p-value	↑/↓	Symbol	Name	Function
1	138	139	123	58	30	44	<0.0001	↓	Ndufs8	NADH dehydrogenase (ubiquinone) Fe-S protein 8 (Complex I)	ox phos
2	18	28	22	7	2	4	0.00002	↓	Ndufab1	NADH dehydrogenase (ubiquinone) 1, alpha/beta subcomplex, 1 (Complex I)	ox phos
3	115	164	130	65	77	71	0.00041	↓	Ndufs4	NADH dehydrogenase (ubiquinone) Fe-S protein 4 (Complex I)	ox phos
4	418	235	270	197	169	183	0.00061	↓	Ndufs1	NADH dehydrogenase (ubiquinone) Fe-S protein 1 (Complex I)	ox phos
5	60	73	61	39	19	29	0.00106	↓	Ndufv1	NADH dehydrogenase (ubiquinone) flavoprotein 1 (Complex I)	ox phos
6	7	21	14	7	2	4	0.00639	↓	Ndufa3	NADH dehydrogenase (ubiquinone) 1 alpha subcomplex, 3 (Complex I)	ox phos
7	41	25	28	18	11	14	0.00780	↓	Ndufb11	NADH dehydrogenase (ubiquinone) 1 beta subcomplex, 11 (Complex I)	ox phos
8	96	99	87	65	65	65	0.01946	↓	Ndufa9	NADH dehydrogenase (ubiquinone) 1 alpha subcomplex, 9 (Complex I)	ox phos
9	149	111	111	113	84	99	0.03128	↓	Ndufa10	NADH dehydrogenase (ubiquinone) 1 alpha subcomplex, 10 (Complex I)	ox phos
10	133	127	115	92	111	102	0.03791	↓	Ndufs2	NADH dehydrogenase (ubiquinone) Fe-S protein 2 (Complex I)	ox phos
11	16	31	23	21	7	14	0.04055	↓	Ndufa6	NADH dehydrogenase (ubiquinone) 1 alpha subcomplex, 6 (B14) (Complex I)	ox phos
12	511	617	514	414	392	403	0.01136	↓	Uqcrc2	ubiquinol cytochrome c reductase core protein 2 (Complex III)	ox phos
13	830	858	754	565	681	623	0.01531	↓	Uqcrc1	ubiquinol cytochrome c reductase core protein 1 (Complex III)	ox phos
14	41	43	38	34	18	26	0.03129	↓	Uqcrq	ubiquinol-cytochrome c reductase subunit VII (Complex III)	ox phos
15	145	130	121	137	86	111	0.04107	↓	Uqcrfs1	ubiquinol-cytochrome c reductase, Rieske iron-sulfur polypeptide 1 (Complex III)	ox phos
16	32	34	30	33	12	23	0.04997	↓	Uqcrh	ubiquinol-cytochrome c reductase hinge protein (Complex III)	ox phos
17	130	127	114	116	90	103	0.04535	↓	Cyc1	cytochrome c-1 (Complex III)	ox phos
18	23	25	22	12	5	9	0.00377	↓	Atp5l	ATP synthase, H+ transporting, mitochondrial F0 complex, (Complex V)	ox phos
19	374	368	329	225	306	266	0.00955	↓	Atp5h	ATP synthase, H+ transporting, mitochondrial F0 complex, (Complex V)	ox phos
20	145	200	160	132	123	128	0.01928	↓	Atp5o	ATP synthase, H+ transporting, mitochondrial F1 complex, (Complex V)	ox phos
21	243	187	185	211	134	172	0.03361	↓	Atp5d	ATP synthase, H+ transporting, mito F1 complex, delta subunit (Complex V)	ox phos
22	216	253	213	109	63	86	<0.0001	↓	Nnt	nicotinamide nucleotide transhydrogenase	FAO
23	436	480	412	196	202	199	<0.0001	↓	Ech1	enoyl coenzyme A hydratase 1	FAO
24	907	870	786	429	458	443	0.00004	↓	Hadhsc	hydroxyacyl-Coenzyme A dehydrogenase, short chain	FAO
25	44	40	37	12	12	12	0.00052	↓	Decr1	dienoyl CoA reductase 1, mitochondrial	FAO
26	91	91	81	46	39	42	0.00078	↓	Slc25a11	solute carrier family 25 (mitochondrial carrier oxoglutarate carrier)	FAO
27	30	42	33	7	16	11	0.00079	↓	Cpt2	carnitine palmitoyltransferase 2	FAO
28	48	55	47	22	23	22	0.00360	↓	Bdh	3-hydroxybutyrate dehydrogenase (heart, mitochondrial)	FAO
29	73	81	69	33	49	41	0.00493	↓	Mte1	mitochondrial acyl-CoA thioesterase 1	FAO
30	398	371	339	302	222	262	0.00507	↓	Acadvl	acyl-Coenzyme A dehydrogenase, very long chain	FAO
31	159	84	100	69	74	71	0.00536	↓	Acads	acyl-Coenzyme A dehydrogenase, short chain	FAO
32	215	218	193	178	121	150	0.00557	↓	Aldh6a1	aldehyde dehydrogenase family 6, subfamily A1	FAO
33	4	16	10	4	2	3	0.00688	↓	Slc25a20	solute carrier family 25 mito carnitine/acylcarnitine translocase)	FAO
34	153	158	139	103	107	105	0.00753	↓	Ivd	isovaleryl coenzyme A dehydrogenase	FAO
35	138	87	94	69	72	71	0.00991	↓	Aldh4a1	aldehyde dehydrogenase 4 family, member A1	FAO
36	83	76	70	54	42	48	0.01323	↓	Hibadh	3-hydroxyisobutyrate dehydrogenase	FAO
37	106	102	92	116	40	78	0.01456	↓	Aldh2	aldehyde dehydrogenase 2, mitochondrial	FAO
38	48	37	37	19	26	23	0.01842	↓	Slc25a12	solute carrier family 25 (mitochondrial carrier, Aralar), member 12	FAO
39	21	24	20	12	9	11	0.02038	↓	Mpst	mercaptopyruvate sulfurtransferase	FAO
40	1226	1302	1133	924	1035	979	0.02749	↓	Hadha	hydroxyacyl-CoA dehydrogenase	FAO
41	174	142	137	148	102	125	0.03191	↓	Them2	thioesterase superfamily member 2	FAO
42	55	37	39	39	19	29	0.03450	↓	Mut	methylmalonyl-Coenzyme A mutase	FAO
43	3	1	2	14	5	10	0.03472	↑	Acate2	acyl-Coenzyme A thioesterase 2, mitochondrial	FAO
44	347	323	295	319	227	273	0.04103	↓	Echs1	enoyl Coenzyme A hydratase, short chain, 1, mitochondrial	FAO
45	40	30	30	25	18	21	0.04634	↓	Acadsb	acyl-Coenzyme A dehydrogenase, short/branched chain	FAO
46	44	46	40	130	86	108	0.04818	↑	Dpysl2	dihydropyrimidinase-like 2	FAO
47	23	19	18	8	12	10	0.02516	↓	Oat	ornithine aminotransferase	AA metab
48	105	88	84	59	42	51	0.00203	↓	Phb	prohibitin	apop
49	42	51	42	41	21	31	0.04783	↓	Pdcd8	programmed cell death 8	apop
50	1121	912	881	705	727	716	0.00962	↓	Hspd1	heat shock protein 1 (chaperonin)	biogen
51	18	22	18	11	9	10	0.03105	↓	Cabc1	chaperone, ABC1 activity of bc1 complex like (S. pombe)	biogen
52	37	37	33	11	16	13	0.00220	↓	Vdac3	voltage-dependent anion channel 3	channel
53	101	75	75	46	51	48	0.00539	↓	Pdhx	pyruvate dehydrogenase complex, component X	glycol/TCA
54	419	468	400	360	357	359	0.04458	↓	Pdhb	pyruvate dehydrogenase (lipoamide) beta	glycol/TCA
55	462	541	455	336	496	416	0.04891	↓	Sod2	superoxide dismutase 2, mitochondrial	ROS metab
56	6	21	14	4	2	3	0.00041	↓	5430428GO1Ri	RIKEN cDNA 5430428G01 gene (unknown)	?
57	216	152	157	95	127	111	0.00157	↓	Chchd3	coiled-coil-helix-coiled-coil-helix domain containing 3	?
58	27	31	26	37	4	20	0.00566	↓	9430083G14Ril	RIKEN cDNA 9430083G14 gene (unknown)	?
59	52	30	34	22	16	19	0.01068	↓	2310005O14Ril	RIKEN cDNA 2310005O14 gene (unknown)	?
60	19	27	21	14	7	10	0.01453	↓	1110013G13Ril	RIKEN cDNA 1110013G13 gene (unknown)	?
R	201	182	192	225	172	199	NS	none	Cox4i1	cytochrome c oxidase subunit IV isoform 1	

The mitochondrial proteins that exhibited significant differences between TG and NTG mice (i.e., LPE ≤ 0.05) are shown, sorted by function. Nos. of spectra observed for each protein, normalized as described in MATERIALS AND METHODS, are shown for the two NTG analyses (*columns 1* and *2*) and the two TG analyses (*columns 4* and *5*). The only proteins shown are those for which at least 1 spectrum was observed in each of the 4 analyses. For reference purposes, the values obtained for cytochrome oxidase IV (Cox4), which did not exhibit any significant difference between NTG and TG samples (see *row 30* in Table 1), are shown in *row R* at the end of the table. *Columns 3* and *6* are the averages of *columns 1* and *2* and of *columns 4* and *5*, respectively. *Column 8* shows whether the value for this protein is increased (↑) or decreased (↓) in TG compared with NTG. *Column 9* shows the gene symbol, and *column 10* shows the gene name and, for the oxidative phosphorylation proteins, the complex to which they belong. *Column 11* shows the function of each protein as follows: ox phos, oxidative phosphorylation; FAO, β-fatty acid oxidation; AA metab, amino acid metabolism; apop, apoptosis; biogen, mitochondrial biogenesis, e.g., protein import; channel, channel protein; glycol/TCA, glycolysis or tricarboxylic acid cycle; ROS metab, reactive oxygen species metabolism; ?, unknown function. All gene symbols and names can be found at Mouse Genome Informatics as http://www.informatics.jax.org/.

proteins were reduced in MKK6 mouse hearts. This suggests that the MKK6 transgenic mouse hearts may exhibit a metabolic switch similar to that observed in failing hearts. The implications of such a switch on myocardial response to I/R are not known. However, it is possible that a switch away from fatty acid to glucose metabolism may be an adaptative response that might allow for the preservation of ATP generation, even though oxidative phosphorylation is reduced.

In addition to the reduced oxidative phosphorylation and FAO proteins, we observed reductions in several proteins involved in apoptosis (prohibitin and programmed cell death 8), as well as the reduction of a mitochondrial channel protein (VDAC3). It is possible that reduced levels of these proteins could contribute to the protective phenotype exhibited by the MKK6 transgenic mouse hearts. However, reduction in the levels of Cabc1, a chaperone involved in mitochondrial biogenesis, and Sod2, which metabolizes mitochondrial matrix ROS, in the transgenic mouse hearts would not be expected to support a more protected phenotype.

Like other proteins, p38 functions in the context of complex networks; therefore, the functional impact of p38 stretches well beyond the scope of our current knowledge. The results of the present study emphasize the extent of what remains to be discovered about the widespread effects of MKK6/p38 activation on the cardiac proteome. As such, proteomic analyses have the potential to identify previously uncharacterized effectors of such pathways and, as demonstrated in the current study, they can lead to new information about how those effectors might contribute to physiologically important phenotypes.

GRANTS

This work was supported by National Institutes of Health Grants HL-63975, NS/HL-25037, and HL-75573 to C. C. Glembotski and a predoctoral fellowship from the American Heart Association to J. J. Martindale.

REFERENCES

1. **Abe J, Baines CP, and Berk BC.** Role of mitogen-activated protein kinases in ischemia and reperfusion injury: the good and the bad. *Circ Res* 86: 607–609, 2000.
2. **Baines CP, Song CX, Zheng YT, Wang GW, Zhang J, Wang OL, Guo Y, Bolli R, Cardwell EM, and Ping P.** Protein kinase Cϵ interacts with and inhibits the permeability transition pore in cardiac mitochondria. *Circ Res* 92: 873–880, 2003.
3. **Barger PM, Browning AC, Garner AN, and Kelly DP.** p38 mitogen-activated protein kinase activates peroxisome proliferator-activated receptor alpha: a potential role in the cardiac metabolic stress response. *J Biol Chem* 276: 44495–44501, 2001.
4. **Bianchi C, Genova ML, Parenti Castelli G, and Lenaz G.** The mitochondrial respiratory chain is partially organized in a supercomplex assembly: kinetic evidence using flux control analysis. *J Biol Chem* 279: 36562–36569, 2004.
5. **Bueno OF and Molkentin JD.** Involvement of extracellular signal-regulated kinases 1/2 in cardiac hypertrophy and cell death. *Circ Res* 91: 776–781, 2002.
6. **Carroll J, Fearnley IM, Shannon RJ, Hirst J, and Walker JE.** Analysis of the subunit composition of complex I from bovine heart mitochondria. *Mol Cell Proteomics* 2: 117–126, 2003.
7. **Chelius D, Zhang T, Wang G, and Shen RF.** Global protein identification and quantification technology using two-dimensional liquid chromatography nanospray mass spectrometry. *Anal Chem* 75: 6658–6665, 2003.
8. **Cossarizza A, Baccarani-Contri M, Kalashnikova G, and Franceschi C.** A new method for the cytofluorimetric analysis of mitochondrial membrane potential using the J-aggregate forming lipophilic cation 5,5′,6,6′-tetrachloro-1,1′,3,3′-tetraethylbenzimidazolcarbocyanine iodide (JC-1). *Biochem Biophys Res Commun* 197: 40–45, 1993.
9. **D'Addario M, Arora PD, Ellen RP, and McCulloch CA.** Interaction of p38 and Sp1 in a mechanical force-induced, beta 1 integrin-mediated transcriptional circuit that regulates the actin-binding protein filamin-A. *J Biol Chem* 277: 47541–47550, 2002.
10. **Degousee N, Martindale J, Stefanski E, Cieslak M, Lindsay TF, Fish JE, Marsden PA, Thuerauf DJ, Glembotski CC, and Rubin BB.** MAP kinase kinase 6-p38 MAP kinase signaling cascade regulates cyclooxygenase-2 expression in cardiac myocytes in vitro and in vivo. *Circ Res* 92: 757–764, 2003.
11. **Di Lisa F, Blank PS, Colonna R, Gambassi G, Silverman HS, Stern MD, and Hansford RG.** Mitochondrial membrane potential in single living adult rat cardiac myocytes exposed to anoxia or metabolic inhibition. *J Physiol* 486: 1–13, 1995.
12. **Fan M, Rhee J, St-Pierre J, Handschin C, Puigserver P, Lin J, Jaeger S, Erdjument-Bromage H, Tempst P, and Spiegelman BM.** Suppression of mitochondrial respiration through recruitment of p160 myb binding protein to PGC-1alpha: modulation by p38 MAPK. *Genes Dev* 18: 278–289, 2004.
13. **Gaballo A, Zanotti F, and Papa S.** Structures and interactions of proteins involved in the coupling function of the protonmotive F(o)F(1)-ATP synthase. *Curr Protein Pept Sci* 3: 451–460, 2002.
14. **Goffart S, von Kleist-Retzow JC, and Wiesner RJ.** Regulation of mitochondrial proliferation in the heart: power-plant failure contributes to cardiac failure in hypertrophy. *Cardiovasc Res* 64: 198–207, 2004.
15. **Guzy RD, Hoyos B, Robin E, Chen H, Liu L, Mansfield KD, Simon MC, Hammerling U, and Schumacker PT.** Mitochondrial complex III is required for hypoxia-induced ROS production and cellular oxygen sensing. *Cell Metab* 1: 401–408, 2005.
16. **Halestrap AP, Clarke SJ, and Javadov SA.** Mitochondrial permeability transition pore opening during myocardial reperfusion–a target for cardioprotection. *Cardiovasc Res* 61: 372–385, 2004.
17. **Herrero A and Barja G.** Sites and mechanisms responsible for the low rate of free radical production of heart mitochondria in the long-lived pigeon. *Mech Ageing Dev* 98: 95–111, 1997.
18. **Hoover HE, Thuerauf DJ, Martindale JJ, and Glembotski CC.** alpha B-crystallin gene induction and phosphorylation by MKK6-activated p38. A potential role for alpha B-crystallin as a target of the p38 branch of the cardiac stress response. *J Biol Chem* 275: 23825–23833, 2000.
19. **Huss JM and Kelly DP.** Mitochondrial energy metabolism in heart failure: a question of balance. *J Clin Invest* 115: 547–555, 2005.
20. **Iuso A, Scacco S, Piccoli C, Bellomo F, Petruzzella V, Trentadue R, Minuto M, Ripoli M, Capitanio N, Zeviani M, and Papa S.** Dysfunctions of cellular oxidative metabolism in patients with mutations in the NDUFS1 and NDUFS4 genes of complex I. *J Biol Chem* 281: 10374–10380, 2006.
21. **Jain N, Thatte J, Braciale T, Ley K, O'Connell M, and Lee JK.** Local-pooled-error test for identifying differentially expressed genes with a small number of replicated microarrays. *Bioinformatics* 19: 1945–1951, 2003.
22. **Jones WK, Brown M, Ren X, He S, and McGuinness M.** NF-kappaB as an integrator of diverse signaling pathways: the heart of myocardial signaling? *Cardiovasc Toxicol* 3: 229–254, 2003.
23. **Kendziorski C, Irizarry RA, Chen KS, Haag JD, and Gould MN.** On the utility of pooling biological samples in microarray experiments. *Proc Natl Acad Sci USA* 102: 4252–4257, 2005.
24. **Liang Q and Molkentin JD.** Redefining the roles of p38 and JNK signaling in cardiac hypertrophy: dichotomy between cultured myocytes and animal models. *J Mol Cell Cardiol* 35: 1385–1394, 2003.
25. **Martindale JJ, Wall JA, Martinez-Longoria DM, Aryal P, Rockman HA, Guo Y, Bolli R, and Glembotski CC.** Overexpression of mitogen-activated protein kinase kinase 6 in the heart improves functional recovery from ischemia in vitro and protects against myocardial infarction in vivo. *J Biol Chem* 280: 669–676, 2005.
26. **Moon SK, Jung SY, and Kim CH.** Transcription factor Sp1 mediates p38MAPK-dependent activation of the p21WAF1 gene promoter in vascular smooth muscle cells by pyrrolidine dithiocarbamate. *Biochem Biophys Res Commun* 316: 605–611, 2004.
27. **Morrison LE, Hoover HE, Thuerauf DJ, and Glembotski CC.** Mimicking phosphorylation of alphaB-crystallin on serine-59 is necessary and sufficient to provide maximal protection of cardiac myocytes from apoptosis. *Circ Res* 92: 203–211, 2003.
28. **Nemoto S, Sheng Z, and Lin A.** Opposing effects of Jun kinase and p38 mitogen-activated protein kinases on cardiomyocyte hypertrophy. *Mol Cell Biol* 18: 3518–3526, 1998.
29. **Novalija E, Kevin LG, Camara AK, Bosnjak ZJ, Kampine JP, and Stowe DF.** Reactive oxygen species precede the epsilon isoform of protein

kinase C in the anesthetic preconditioning signaling cascade. *Anesthesiology* 99: 421–428, 2003.
30. **Novalija E, Varadarajan SG, Camara AK, An J, Chen Q, Riess ML, Hogg N, and Stowe DF.** Anesthetic preconditioning: triggering role of reactive oxygen and nitrogen species in isolated hearts. *Am J Physiol Heart Circ Physiol* 283: H44–H52, 2002.
31. **Petrich BG and Wang Y.** Stress-activated MAP kinases in cardiac remodeling and heart failure; new insights from transgenic studies. *Trends Cardiovasc Med* 14: 50–55, 2004.
32. **Ping P and Murphy E.** Role of p38 mitogen-activated protein kinases in preconditioning: a detrimental factor or a protective kinase? *Circ Res* 86: 921–922, 2000.
33. **Ravingerova T, Barancik M, and Strniskova M.** Mitogen-activated protein kinases: a new therapeutic target in cardiac pathology. *Mol Cell Biochem* 247: 127–138, 2003.
34. **Sack MN, Disch DL, Rockman HA, and Kelly DP.** A role for Sp and nuclear receptor transcription factors in a cardiac hypertrophic growth program. *Proc Natl Acad Sci USA* 94: 6438–6443, 1997.
35. **Sack MN, Rader TA, Park S, Bastin J, McCune SA, and Kelly DP.** Fatty acid oxidation enzyme gene expression is downregulated in the failing heart. *Circulation* 94: 2837–2842, 1996.
36. **Sayen MR, Gustafsson AB, Sussman MA, Molkentin JD, and Gottlieb RA.** Calcineurin transgenic mice have mitochondrial dysfunction and elevated superoxide production. *Am J Physiol Cell Physiol* 284: C562–C570, 2003.
37. **Schagger H, Brandt U, Gencic S, and von Jagow G.** Ubiquinol-cytochrome-c reductase from human and bovine mitochondria. *Methods Enzymol* 260: 82–96, 1995.
38. **Schagger H, Noack H, Halangk W, Brandt U, and von Jagow G.** Cytochrome-*c* oxidase in developing rat heart enzymic properties and amino-terminal sequences suggest identity of the fetal heart and the adult liver isoform. *Eur J Biochem* 230: 235–241, 1995.
39. **Scheubel RJ, Tostlebe M, Simm A, Rohrbach S, Prondzinsky R, Gellerich FN, Silber RE, and Holtz J.** Dysfunction of mitochondrial respiratory chain complex I in human failing myocardium is not due to disturbed mitochondrial gene expression. *J Am Coll Cardiol* 40: 2174–2181, 2002.
40. **Stanley WC and Chandler MP.** Energy metabolism in the normal and failing heart: potential for therapeutic interventions. *Heart Fail Rev* 7: 115–130, 2002.
41. **St-Pierre J, Buckingham JA, Roebuck SJ, and Brand MD.** Topology of superoxide production from different sites in the mitochondrial electron transport chain. *J Biol Chem* 277: 44784–44790, 2002.
42. **Sugden PH and Clerk A.** "Stress-responsive" mitogen-activated protein kinases (c-Jun N-terminal kinases and p38 mitogen-activated protein kinases) in the myocardium. *Circ Res* 83: 345–352, 1998.
43. **Taegtmeyer H.** Energy metabolism of the heart: from basic concepts to clinical applications. *Curr Probl Cardiol* 19: 59–113, 1994.
44. **Turrens JF.** Superoxide production by the mitochondrial respiratory chain. *Biosci Rep* 17: 3–8, 1997.
45. **Vogel RO, Janssen RJ, Ugalde C, Grovenstein M, Huijbens RJ, Visch HJ, van den Heuvel LP, Willems PH, Zeviani M, Smeitink JA, and Nijtmans LG.** Human mitochondrial complex I assembly is mediated by NDUFAF1. *FEBS J* 272: 5317–5326, 2005.
46. **Wang Y.** Signal transduction in cardiac hypertrophy—dissecting compensatory versus pathological pathways utilizing a transgenic approach. *Curr Opin Pharmacol* 1: 134–140, 2001.
47. **Wang Y, Huang S, Sah VP, Ross J Jr, Brown JH, Han J, and Chien KR.** Cardiac muscle cell hypertrophy and apoptosis induced by distinct members of the p38 mitogen-activated protein kinase family. *J Biol Chem* 273: 2161–2168, 1998.
48. **Washburn MP, Wolters D, and Yates JR III.** Large-scale analysis of the yeast proteome by multidimensional protein identification technology. *Nat Biotechnol* 19: 242–247, 2001.
49. **Wei J, Sun J, Yu W, Jones A, Oeller P, Keller M, Woodnutt G, and Short J.** Global proteome discovery using an online three-dimensional LC-MS/MS. *J Proteome Res* 4: 801–808. 2005.
50. **Wen JJ and Garg N.** Oxidative modification of mitochondrial respiratory complexes in response to the stress of *Trypanosoma cruzi* infection. *Free Radic Biol Med* 37: 2072–2081, 2004.
51. **Wolters DA, Washburn MP, and Yates JR III.** An automated multidimensional protein identification technology for shotgun proteomics. *Anal Chem* 73: 5683–5690, 2001.
52. **Wu X, Zimmerman GA, Prescott SM, and Stafforini DM.** The p38 MAPK pathway mediates transcriptional activation of the plasma platelet-activating factor acetylhydrolase gene in macrophages stimulated with lipopolysaccharide. *J Biol Chem* 279: 36158–36165, 2004.
53. **Yasmin W, Strynadka KD, and Schulz R.** Generation of peroxynitrite contributes to ischemia-reperfusion injury in isolated rat hearts. *Cardiovasc Res* 33: 422–432, 1997.
54. **Zechner D, Craig R, Hanford DS, McDonough PM, Sabbadini RA, and Glembotski CC.** MKK6 activates myocardial cell NF-kappaB and inhibits apoptosis in a p38 mitogen-activated protein kinase-dependent manner. *J Biol Chem* 273: 8232–8239, 1998.
55. **Zechner D, Thuerauf DJ, Hanford DS, McDonough PM, and Glembotski CC.** A role for the p38 mitogen-activated protein kinase pathway in myocardial cell growth, sarcomeric organization, and cardiac-specific gene expression. *J Cell Biol* 139: 115–127, 1997.
56. **Zeeberg BR, Feng W, Wang G, Wang MD, Fojo AT, Sunshine M, Narasimhan S, Kane DW, Reinhold WC, Lababidi S, Bussey KJ, Riss J, Barrett JC, and Weinstein JN.** GoMiner: a resource for biological interpretation of genomic and proteomic data. *Genome Biol* 4: R28, 2003.